Characterization of three episodic ataxia mutations in the human Kv1.1 potassium channel

Patricia Zerr[a], John P. Adelman[a,*], James Maylie[b]

[a] *Vollum Institute, Oregon Health Sciences University, L-474, 3181 S.W. Sam Jackson Park Road, Portland, OR 97201, USA*
[b] *Department of Obstetrics and Gynecology, Oregon Health Sciences University, Portland, OR 97201, USA*

Received 17 June 1998

Abstract Episodic ataxia (EA) is a rare inherited neurological disorder due to mutation in the voltage-dependent Kv1.1 potassium channel. In nine unrelated families, a different missense point mutation at highly conserved positions has been reported. We have previously characterized six of the EA mutants. In this study, three recently identified mutations were introduced into the human Kv1.1 cDNA and expressed in *Xenopus* oocytes. Compared to wild type, T226A and T226M reduced the current amplitude by >95%, shifted the voltage dependence by 15 mV, and slowed activation and deactivation kinetics. Currents from G311S were ~25% of wild type, less steeply voltage-dependent and had more pronounced C-type inactivation. These altered gating properties will reduce the delayed-rectifier potassium current which may underlie the symptoms of EA.

Key words: Ataxia; Potassium channel; Kv1.1; Inherited disease

1. Introduction

Episodic ataxia type 1 (EA-1) is a rare autosomal dominant neurological disorder characterized by brief attacks of imbalance and impaired movements [1]. Attacks usually last several minutes and are often induced by physical or emotional stress. The frequency (from several times a day to once a month) and the severity of the attacks vary between and within affected families. In addition to ataxia, affected individuals exhibit myokymia which is caused by abnormal peripheral nerve function [2]. Genetic linkage studies have identified the gene encoding the voltage-gated delayed-rectifier potassium channel Kv1.1 (*KCNA1*) as underlying the inherited form of EA [3,4]. In each of nine families, a different single missense point mutation was identified in the coding sequence of Kv1.1, and all affected individuals are heterozygous [3–6]. All mutations affect amino acids which are invariant in the *KCNA1* coding sequence from human, rat, mouse and the *Drosophila Shaker* gene, as well as among other members of the human Kv1 subfamily. Conservation of these residues through evolution suggests that they are important for normal channel function.

In previous work, we have studied six of the EA mutants by expression in *Xenopus* oocytes, and showed that five of them form functional homomeric channels with altered biophysical properties compared to wild type, while one was non-functional. EA subunits are also able to coassemble with wild type subunits and the resulting heteromeric channels have phenotypes intermediate between the individual homomeric EA and wild type channels [7,8]. The present report describes the functional characterization of three more recently identified EA mutations: T226A [6], T226M [5] and G311S (M. Litt, personal communication).

2. Materials and methods

Xenopus care and handling were in accordance with the highest standards of institutional guidelines. Frogs underwent no more than two surgeries separated by at least 3 weeks. Before surgery, frogs were anesthetized with an aerated solution of 3-aminobenzoic acid ethyl ester.

EA mutations were introduced into the human Kv1.1 cDNA using a site-directed mutagenesis procedure based on PCR with the proofreading Pfu DNA polymerase (Stratagene) followed by the digestion of the PCR reaction with *Dpn*I [9]. In vitro mRNA synthesis and rigorous quantification were performed as previously described [7]. *Xenopus* oocytes were injected with mRNA and incubated at 18°C in ND96 containing (in mM): 96 NaCl, 2 KCl, 1 $MgCl_2$, 1.8 $CaCl_2$, 10 HEPES, 2.5 Na-pyruvate, 0.5 theophylline, and 10 μg/ml gentamicin, pH 7.5. Currents were recorded 3–6 days following injection in recording solution which was ND96 without gentamicin, theophylline and Na-pyruvate. Two-electrode voltage clamp recordings were performed at room temperature with a Geneclamp 500 amplifier (Axon Instruments) interfaced to a Macintosh Quadra 800 computer. Data were collected and analyzed using Pulse/PulseFit (Heka) and IGOR (Wavemetrics) softwares. Linear leak and capacitance currents were corrected with a P/4 leak subtraction procedure. Statistical significance was determined by an unpaired Student's *t*-test, and $P < 0.01$ was considered significant.

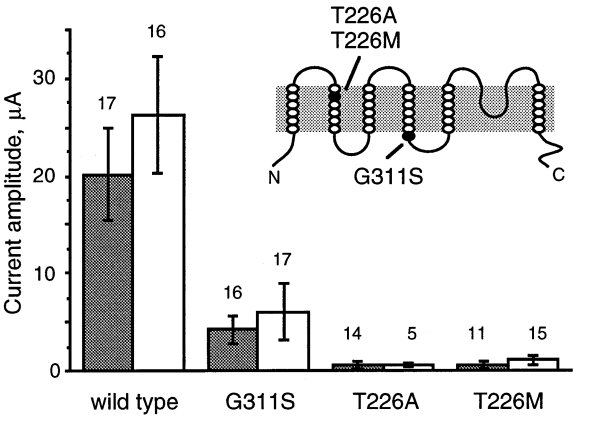

Fig. 1. EA mutants form functional homomeric channels. Amplitudes of steady-state currents recorded at 40 mV from oocytes injected with equal amounts of wild type, T226A, T226M or G311S mRNAs. Data from two independent experiments performed on different batches of oocytes are illustrated in white and gray columns. Error bars represent S.D., and numbers above the columns represent number of cells recorded. Positions of the EA mutations in the Kv1.1 subunit are shown in the inset.

*Corresponding author. Fax: (1) (503) 494 4353.
E-mail: adelman@ohsu.edu

PII: S0014-5793(98)00814-X

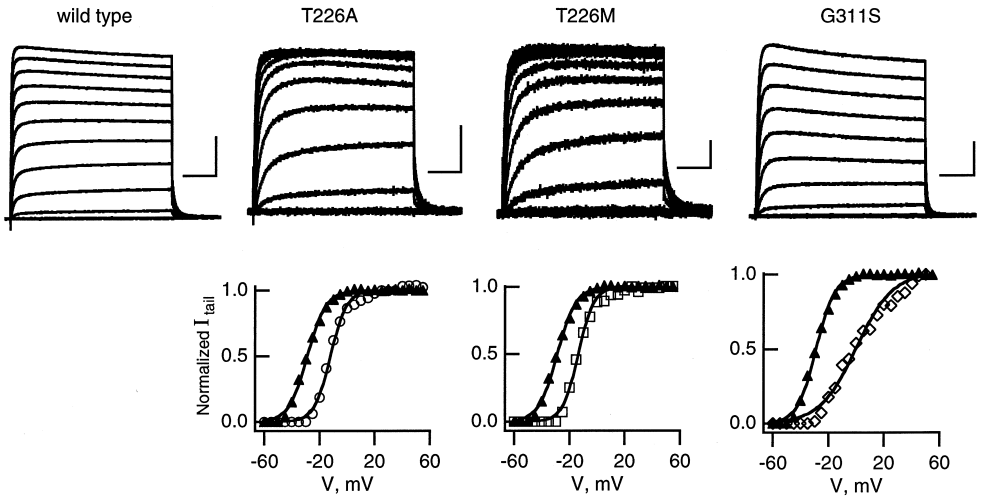

Fig. 2. Voltage dependence of activation. Top panels: Representative families of current traces for wild type and EA mutants evoked from −60 to 50 mV, in 10 mV increments. The holding potential was −80 mV and tail currents were recorded at −50 mV. Horizontal calibration bracket: 100 ms; vertical calibration bracket: 5 μA for wild type, 0.5 μA for T226A, 0.2 μA for T226M and 1 μA for G311S. Lower panels: Normalized tail currents (I_{tail}: amplitude of the exponential that fits the tail current) determined from the current traces illustrated above (wild type (▲), T226A (○), T226M (□), G311S (◇)) are represented as a function of the voltage of the depolarizing test pulse. Data points were fitted according to the Boltzmann equation $I = 1/(1+\exp((V-V_{1/2})/k))$, where $V_{1/2}$ is the potential of half-activation and k is the slope factor.

3. Results

The positions of T226 and G311 in the human Kv1.1 subunit are shown on the transmembrane topology representation illustrated in the inset in Fig. 1. T226 is located in the second transmembrane domain and G311 at the intracellular C-terminus of S4. These residues are located in different domains than the previously characterized EA mutations [7,10]. T226A, T226M and G311S were introduced into the human Kv1.1 cDNA, and equal amounts of wild type or EA mRNA (see methods [7]) were injected into *Xenopus* oocytes. Currents were studied 3–6 days later with the two-electrode voltage clamp technique. Fig. 1 compares wild type and EA steady-state currents recorded at 40 mV. Results from two independent experiments (gray and white columns) performed on different batches of oocytes are shown. The three EA subunits formed functional homomeric channels, but currents were markedly reduced compared to wild type. G311S yielded currents that were ∼25% of wild type. T226A and T226M had an even more drastic effect, currents being ≤5% of wild type (Table 1). To determine whether the functional properties of the channels were affected, the voltage dependence and kinetics of EA currents were investigated and compared to wild type.

3.1. T226A and T226M

T226A and T226M are substitutions at the same position; in both cases, the hydroxyl side chain of threonine is replaced by a hydrophobic side chain. Families of currents were measured with test potentials ranging from −50 mV to 60 mV, in 10 mV increments, from a holding potential of −80 mV (Fig. 2, upper panel). The voltage dependence of activation was determined from tail currents measured upon repolarization to −50 mV following each test pulse. Tail currents were fitted with a single exponential and the amplitude of the exponential plotted as a function of the test potential. Data points were fitted with a Boltzmann equation to determine the potential of half-maximal activation, $V_{1/2}$, and the slope factor, or steepness of voltage dependence, k. Both T226A and T226M shifted $V_{1/2}$ by ∼15 mV to more positive potentials (Fig. 2, lower panel, Table 1). The slope factor was 6.0 ± 0.5 mV ($n = 7$) and 6.1 ± 0.7 mV ($n = 10$) for T226A and T226M, respectively, compared to 8.1 ± 0.9 mV ($n = 6$) for wild type. These values were slightly but nevertheless significantly reduced ($P < 0.01$, Student's t-test), suggesting an increased voltage dependence for these EA mutants.

The effects of T226A and T226M on activation and deactivation kinetics were also investigated. Activation kinetics were determined by fitting the rising phase of current traces

Table 1
Biophysical parameters of homomeric wild type and EA mutants

	Relative amplitude	Voltage-dependent parameters		Activation		Deactivation		C-type inactivation
		$V_{1,2}$ (mV)	k (mV)	$\tau_{V1/2}$ (ms)	k (mV)	$\tau_{V1/2}$ (ms)	k (mV)	I_{final}/I_{peak}
Wild type	100.0	−28.8 ± 2.3 (6)	8.1 ± 0.9	14.6 ± 3.7 (5)	30.1 ± 2.8	22.8 ± 2.3 (5)	26.6 ± 2.5	0.70 ± 0.01 (10)
T226A	2.4	−14.5 ± 2.1 (7)*	6.0 ± 0.5*	26.0 ± 3.6 (7)*	31.2 ± 2.0	51.2 ± 16.3 (6)*	21.0 ± 1.9*	0.69 ± 0.03 (8)
T226M	3.9	−14.0 ± 2.1 (10)*	6.1 ± 0.7*	24.0 ± 6.3 (9)*	33.6 ± 3.3	65.0 ± 10.6 (10)*	20.0 ± 1.6*	0.70 ± 0.03 (6)
G311S	22.9	2.9 ± 2.7 (8)*	13.4 ± 0.8*	14.2 ± 2.4 (4)	47.8 ± 2.7*	20.7 ± 5.2 (8)	35.0 ± 3.6*	0.52 ± 0.03 (8)*

Steady-state current amplitudes measured at 40 mV are given as percent of wild type which was 20.2 ± 4.7 μA ($n = 17$). Voltage-dependent parameters of activation ($V_{1/2}$ and k) were obtained from the Boltzmann equation described in Fig. 2. Activation and deactivation time constants at $V_{1/2}$ and the corresponding slope factors, k, were derived as described from Fig. 3. C-type inactivation was measured at 20 mV and is presented as the ratio I_{final}/I_{peak}. Data are presented as means ± S.D. (number of cells). Asterisks represent significance of $P < 0.01$ compared to wild type.

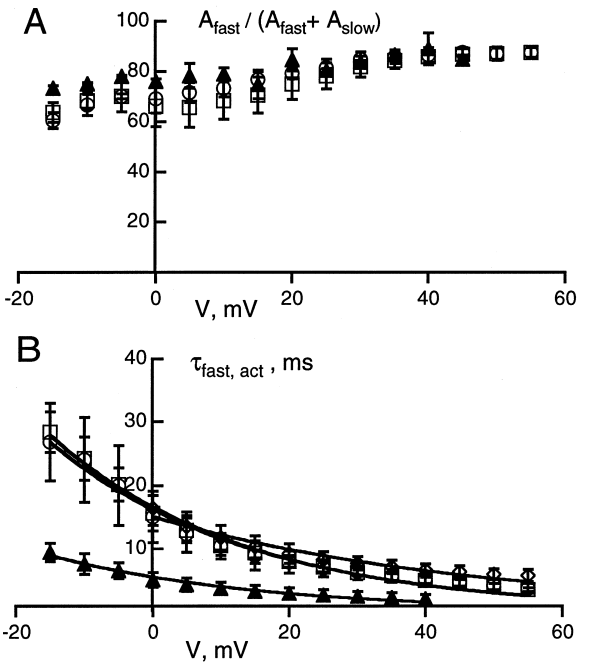

Fig. 3. Activation kinetics of wild type and EA currents. A: The rising phase of wild type, T226A and T226M currents was best fitted with the sum of two exponentials. The relative contribution of the fast component, represented by the fraction $A_{fast}/(A_{fast}+A_{slow})$, where A_{fast} and A_{slow} are the amplitude of the fast and the slow exponentials respectively, were plotted as a function of test potential for wild type (▲, $n=5$), T226A (○, $n=7$) and T226M (□, $n=9$). B: Representation of the time constant of the fast exponential ($\tau_{fast,act}$) for wild type (▲, $n=5$), T226A (○, $n=7$) and T226M (□, $n=9$) and of the time constant of the single exponential describing the activation of G311S (◇, $n=4$) as a function of the potential. Data points were fitted according to the equation $\tau=\tau_{V1/2}\exp((V-V_{1/2})/k)$, where $\tau_{V1/2}$ is the time constant of activation at $V_{1/2}$ and k is the slope factor for the voltage dependence of the time constants. Symbols and error bars represent mean ± S.D.

similar to those illustrated in Fig. 2 for test potentials >-20 mV. Over the complete voltage range, current traces were best fitted with a sum of two exponentials. The fast component accounted for from 70% at lower potentials to 90% at more depolarized potentials (Fig. 3A). The fast exponential being dominant, its time constant, $\tau_{fast,act}$, was plotted versus voltage pulse (Fig. 3B). At a given potential, T226A and T226M activated ~2 times slower than wild type. To see whether the shift in the voltage dependence of activation reported above could explain the slower kinetics, $\tau_{fast,act}$ was determined at $V_{1/2}$ by fitting the data to an exponential function (Fig. 3B); taking in account the shift in $V_{1/2}$, T226A and T226M activated more slowly than wild type (Table 1). These results indicate significant changes in the gating of the T226A and T226M channels.

Deactivation rates were determined by measuring tail currents from −30 to −80 mV after a 100 ms step pulse to 40 mV (Fig. 4A). Tail currents were fitted with a single exponential and the time constant of deactivation, τ_{deact}, was plotted as a function of the potential (Fig. 4B). Similar to activation kinetics, when compared at $V_{1/2}$, τ_{deact} were ~2–3 times slower for T226A and T226M than for wild type (Table 1), suggesting a decreased first closing transition of these EA channels [11].

C-type inactivation was also evaluated by activating the channel for 10 s to voltage steps between −20 and 60 mV, in 20 mV increments. Representative current traces at 0 mV are shown in Fig. 5A; to compare the time course of the EA channels to wild type, currents are normalized to their maximal amplitude. C-type inactivation was quantified by measuring the peak current (I_{peak}) and the current at the end of the pulse (I_{final}). The ratio, I_{final}/I_{peak}, shows that T226A and T226M did not affect C-type inactivation; neither its voltage independence, as shown for the *Shaker* channel [12], nor the ratio I_{final}/I_{peak} (~0.7) was changed (Fig. 5B, Table 1).

3.2. G311S

Representative currents recorded from an oocyte injected with G311S mRNA are shown in Fig. 2 (upper panel), as well as the corresponding activation curve (lower panel). Data analyses showed that the voltage dependence of activation for G311S was shifted by ~30 mV (Table 1). The slope of the activation curve was more shallow; $k=13.4\pm0.8$ mV ($n=8$) for G311S compared to 8.1 ± 0.9 mV ($n=6$) for wild type, indicating that G311S has a reduced voltage dependence of activation.

In contrast to wild type, T226A, and T226M, the rising phase of G311S currents was best fitted with a single exponential. The τ_{act} for G311S was slower than $\tau_{fast,act}$ for wild type throughout the range of potentials tested (Fig. 3B). However, when compared at $V_{1/2}$, the time constants were not significantly different (Table 1), indicating that the shift in the voltage dependence of activation for G311S can, by itself, explain the slower τ_{act} at a given potential.

Similarly, deactivation kinetics of G311S, determined from tail currents as described above, were not significantly different from wild type when compared at $V_{1/2}$ (Table 1).

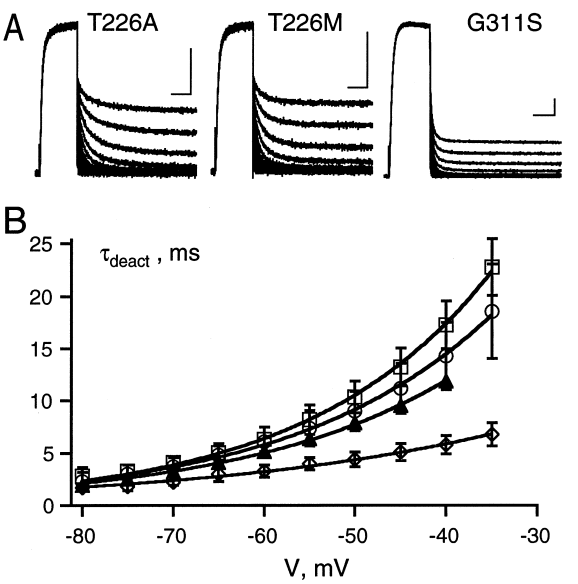

Fig. 4. Voltage dependence of deactivation kinetics. A: Deactivation was determined at potentials from −10 to −80 mV (increments of −5 mV) following the activation of the current at 40 mV for 100 ms. Representative currents recorded with this protocol for T226A, T226M and G311S are shown. Horizontal and vertical calibration brackets: 50 ms and 0.5 μA respectively. B: Representation of the time constant of deactivation (τ_{deact}) for wild type (▲, $n=5$), T226A (○, $n=6$), T226M (□, $n=10$) and G311S (◇, $n=8$) as a function of the tail potential. Data points were fitted as described in the legend to Fig. 3 to determine the time constant of deactivation at $V_{1/2}$. Symbols and error bars represent mean ± S.D.

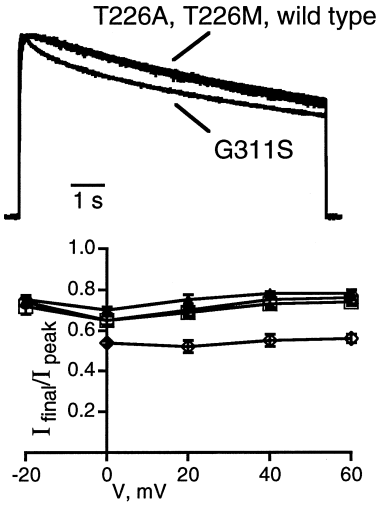

Fig. 5. C-type inactivation of EA mutants. A: Superimposed normalized current traces from T226A, T226M, G311S and wild type. The membrane potential was depolarized from −80 mV to 0 mV for 10 s. B: Representation of the amount of C-type inactivation (I_{final}/I_{peak}) for T226A (○, $n=8$), T226M (□, $n=6$) and G311S (◇, $n=8$) as a function of the voltage. Symbols and error bars represent mean ± S.D.

C-type inactivation was clearly faster for G311S (Fig. 5A). At the end of a 10 s pulse, the current amplitude was about half of the initial amplitude. C-type inactivation was voltage-independent, as I_{final}/I_{peak} was constant from 0 to 60 mV (Fig. 5B).

4. Discussion

Three recently reported EA mutations in Kv1.1 have been shown to form functional homomeric channels with reduced currents and altered biophysical properties when compared to wild type.

T226A and T226M yielded currents that were ≤5% of wild type; both mutations shifted the threshold of activation and slowed the activation and deactivation kinetics at $V_{1/2}$. The magnitude of these effects was similar for T226A and T226M. Alanine and methionine have different hydrophobic cores, however, this does not seem to affect the current, since the two channels are functionally indistinguishable. On the other hand, both residues are neutral non-polar amino acids. Given the remarkable conservation of T226, it seems that the polarity of the hydroxyl-bearing side chain of threonine is crucial for the normal function of Kv1.1 channels, possibly through formation of a hydrogen bond with another residue.

Currents evoked from G311S channels were ~25% of wild type current amplitudes. The potential of half-activation was shifted to more positive potentials and channels were less voltage-sensitive. Activation and deactivation kinetics at $V_{1/2}$ were not affected. However, the C-type inactivation was faster. A more shallow current-voltage relationship signifies a reduced voltage sensitivity, suggesting the movement of fewer charges is necessary to activate the channel. Interestingly, G311S is located at the C-terminal end of S4, the major element of the voltage sensor [13–15], and because of its position might affect the mobility of the voltage sensor, or the coupling of the voltage sensor to the gate. G311S also undergoes faster C-type inactivation than wild type. Residues in the outer vestibule of the pore contribute to C-type inactivation [16,17]. In contrast, the three EA residues that we have found to increase C-type inactivation, G311S, E325D and V408A [7], are all located on the intracellular side of the pore, suggesting that this region of the channel is also involved in slow inactivation.

Besides the biophysical characterization of homomeric T226A, T226M and G311S channels described in this report, the cellular and molecular mechanisms by which the three alleles cause an alteration of channel function need yet to be determined. All EA patients are heterozygous and if both wild type and the EA alleles are active, it is expected that wild type and EA subunits coassemble to form heteropolymeric channels with affected functions. For the three mutations described here, currents are markedly reduced, and this might affect the delayed-rectifier current density, a haploinsufficiency effect. Also, biophysical properties of homomeric EA channels are abnormal and these may be conferred, at least in part, on heteromeric channels which incorporate EA subunits, a dominant negative effect. These mutations are responsible for the EA syndrome and the understanding of the molecular pathogenesis of the disease will possibly lead to treatments of this neurological disorder. Additionally, the naturally occurring EA mutations can be used as structure-function probes for the study of voltage activated K channels.

References

[1] Ashizawa, T., Butler, I.J., Harati, Y. and Roongta, S.M. (1983) Ann. Neurol. 13, 285–290.
[2] Brunt, E.R. and Tiemen, V.W. (1990) Brain 113, 1361–1382.
[3] Browne, D.L., Gancher, S.T., Nutt, J.G., Brunt, E.R.P., Smith, E.A., Kramer, P. and Litt, M. (1994) Nature Genet. 8, 136–140.
[4] Browne, D.L., Brunt, E.R.P., Griggs, R.C., Nutt, J.G., Gancher, S.T., Smith, E.A. and Litt, M. (1995) Hum. Mol. Genet. 4, 1671–1672.
[5] Çomu, S., Giuliani, M. and Narayanan, V. (1996) Am. Ann. Assoc. 48, 684–687.
[6] Sheffer, H., Brunt, E.R.P., Mol, G.J.J., Van der Vlies, P., Stulp, R.P., Verlind, E., Mantel, G., Averyanov, Y.N., Hofstra, R.M.W. and Buys, C.H.C. (1998) Hum. Genet. 102, 464–466.
[7] Zerr, P., Adelman, J.P. and Maylie, J. (1998) J. Neurosci. 18, 2842–2848.
[8] D'Amado, C.M., Liu, Z.P., Adelman, J.P., Maylie, J. and Pessia, M. (1998) EMBO J. 17, 1200–1207.
[9] Ishii, T.M., Zerr, P., Xia, X.M., Bond, C., Maylie, J. and Adelman, J.P. (1998) Methods Enzymol. (in press).
[10] Adelman, J.P., Bond, C., Pessia, M. and Maylie, J. (1995) Neuron 15, 1449–1454.
[11] Zagotta, W.N., Hoshi, T., Dittman, J. and Aldrich, R.W. (1994) J. Gen. Physiol. 103, 279–319.
[12] Hoshi, T., Zagotta, W.N. and Aldrich, R.W. (1991) Neuron 7, 547–556.
[13] Tytgat, J., Nakazawa, K., Gross, A. and Hess, P. (1993) J. Biol. Chem. 268, 23777–23779.
[14] Plannels-Cases, R., Ferrer-Montiel, A.V., Patten, C.D. and Montal, M. (1995) Proc. Natl. Acad. Sci. USA 92, 9422–9426.
[15] Aggarwal, S.K. and MacKinnon, R. (1996) Neuron 16, 1169–1177.
[16] Braukowitz, T. and Yellen, G. (1995) Neuron 15, 951–960.
[17] Molina, A., Castellano, A.G. and Lopez-Barneo, J. (1997) J. Physiol. 499, 361–367.